



Separating refractory and non-refractory
particulate chloride

I. Nuaaman et al.

Separating refractory and non-refractory particulate chloride and estimating chloride depletion by aerosol mass spectrometry in a marine environment

I. Nuaaman^{1,2}, S.-M. Li², K. L. Hayden², T. B. Onasch³, P. Massoli³, D. Sueper³,
D. R. Worsnop³, T. S. Bates^{4,5}, P. K. Quinn⁵, and R. McLaren¹

¹Center for Atmospheric Chemistry, York University, Toronto, Ontario, Canada

²Air Quality Research Division, Science and Technology Branch, Environment Canada,
Downsview, Ontario, Canada

³Aerodyne Research, Billerica, Massachusetts, USA

⁴Joint Institute for the Study of the Atmosphere and Ocean, University of Washington, Seattle,
USA

⁵Pacific Marine Environmental Laboratory, NOAA, Seattle, Washington, USA

Received: 10 December 2014 – Accepted: 22 December 2014 – Published: 22 January 2015

Correspondence to: S.-M. Li (shao-meng.li@ec.gc.ca) and R. McLaren (rmclaren@yorku.ca)

Published by Copernicus Publications on behalf of the European Geosciences Union.

Title Page

Abstract

Introduction

Conclusions

References

Tables

Figures



Back

Close

Full Screen / Esc

Printer-friendly Version

Interactive Discussion



Abstract

Aerosol composition and concentration measurements along the coast of California were obtained using an Aerodyne high-resolution time-of-flight aerosol mass spectrometer (HR-AMS) onboard the research vessel *Atlantis* during the CalNex study in 2010. This paper focuses on the measurement of aerosol chloride using the HR-AMS that can be ambiguous in regions with significant quantities of sea salt aerosols. This ambiguity arises due to large differences in the sensitivity of the HR-AMS to refractory chloride species (i.e., NaCl) and non refractory chloride species (i.e., NH₄Cl, HCl, etc.). Using the HR-AMS, the aerosol chloride signal is typically quantified using ion signals for ³⁵Cl⁺, H³⁵Cl⁺, ³⁷Cl⁺ and H³⁷Cl⁺ (H_xCl⁺). During this study, the highest aerosol chloride signal was observed during sea sweep experiments when the source of the aerosol chloride was NaCl present in artificially generated sea salt aerosols even though the HR-AMS has significantly lower sensitivity to such refractory species. Other prominent ion signals that arise from NaCl salt were also observed at *m/z* 22.99 for Na⁺ and *m/z* 57.96 for Na³⁵Cl⁺ during both sea sweep experiments and during periods of ambient measurements. Thus, refractory NaCl contributes significantly to the H_xCl⁺ signal, interfering with attempts to quantify non sea salt chloride (nssCl). It was found that during ambient aerosol measurements, the interference in the H_xCl⁺ signal from sea salt chloride (ssCl) was as high as 89%, but with a study wide average of 10%. The Na³⁵Cl⁺ ion signal was found to be a good tracer for NaCl. We outline a method to establish nssCl in the ambient aerosols by subtracting the sea salt chloride (ssCl) signal from the H_xCl⁺ signal. The ssCl signal is derived from the Na³⁵Cl⁺ ion tracer signal and the H_xCl⁺ to Na³⁵Cl⁺ ratio established from the sea sweep experiments. Ambient submicron concentrations of ssCl were also established using the Na³⁵Cl⁺ ion tracer signal and a scaling factor determined through simultaneous measurements of submicron aerosol chloride on filters. This scaling factor accounts for the low vaporization response of the AMS heater to ssCl, although regular calibration of this response is recommended in future applications. It follows that true total particulate chloride (pCl)

Separating refractory and non-refractory particulate chloride

I. Nuaaman et al.

Title Page

Abstract

Introduction

Conclusions

References

Tables

Figures



Back

Close

Full Screen / Esc

Printer-friendly Version

Interactive Discussion



is the sum of nssCl and ssCl. In this study, the median levels observed for the concentrations of pCl, nssCl and ssCl were 0.052, 0.017 and 0.024 $\mu\text{g m}^{-3}$ respectively. The average contributions of nssCl and ssCl to pCl were 48 and 52 % respectively, with nssCl dominating in periods of continental outflow and ssCl dominating during other periods. Finally, we propose a method to measure percentage chloride depletion of NaCl in ambient submicron sea salt aerosols, strictly using the AMS measurements of Na^+ and $\text{Na}^{35}\text{Cl}^+$ ion signals. The median chloride depletion in submicron aerosols in this study was found to be 78 %.

1 Introduction

Atmospheric aerosols can have an adverse effect on human health, and elevated aerosol concentrations have been linked to increased morbidity and mortality (Lippmann et al., 2000; Cai and Griffin, 2006). Aerosols also impact the Earth's climate through direct and indirect effects on the radiative balance (Solomon et al., 2007) and can cause significant reduction of visibility in polluted areas (Watson, 2002)

Inorganic aerosols typically constitute 25–50 % of the total aerosol submicron mass. Particulate chloride (pCl) can be a major component in coastal and marine aerosols (Moya et al., 2002, and references therein). Sources of pCl are both primary and secondary in nature, where the former refers to sources that lead to direct emissions of pCl into the atmosphere and the latter occurs as a result of chemical and physical processes including gas to aerosol conversion (Pio and Harrison, 1987; Wexler and Seinfeld, 1990). Wind-induced bubble bursting at the ocean surface, which generates sea salt aerosols, is the most significant source of pCl on a global scale (Keene et al., 1999). Other primary sources of inorganic chloride, from crustal dust, refuse burning and biomass burning are insignificant by comparison (Keene et al., 1999). The main sink of sea salt aerosols is deposition, with a relatively short lifetime of 1.5 days since sea salt aerosols exist mostly in the supermicron size range (Keene et al., 1999, and references therein). Secondary particulate chloride can arise from the reversible forma-

Separating refractory and non-refractory particulate chloride

I. Nuaaman et al.

Title Page

Abstract

Introduction

Conclusions

References

Tables

Figures



Back

Close

Full Screen / Esc

Printer-friendly Version

Interactive Discussion



tion of ammonium chloride (NH_4Cl) in the solid (s) and aqueous (aq) phases. NH_4Cl (s, aq) is in equilibrium with its gaseous precursors hydrochloric acid (HCl) and ammonia (NH_3),:



5 Regional sources of ammonia in California arise mainly from dairy farms and automobiles that are equipped with three-way catalytic converters (Neuman, 2003; Docherty et al., 2008; Livingston et al., 2009; Nowak et al., 2012; Hersey et al., 2013). The formation of particle phase NH_4Cl is dependent on temperature, relative humidity (RH), aerosol chemical composition, and the partial pressures of both HCl and NH_3 . The
10 formation of $\text{NH}_4\text{Cl}_{(\text{s, aq})}$ is favorable under conditions of low temperatures and high RH (Pio and Harrison, 1987; Wexler and Seinfeld, 1990; Matsumoto and Tanaka, 1996; Trebs et al., 2005; Ianniello et al., 2011). Furthermore, the partitioning of NH_4Cl to the aerosol phase is reported to be dependent on the availability of excess NH_3 after the neutralization of H_2SO_4 to form $(\text{NH}_4)_2\text{SO}_4$, since the affinity of NH_3 for H_2SO_4 is
15 higher than its affinity for HCl (Trebs et al., 2005; Ianniello et al., 2011).

HCl is emitted directly in the atmosphere from biomass burning, coal combustion and waste incineration (Andreae et al., 1996; McCulloch et al., 1999; Ianniello et al., 2011). Significant amounts of gaseous HCl are also produced from acid displacement of chloride from sea salt aerosols. This acid displacement is driven by nitric acid, sulfuric acid (Finalyson-Pitts and Pitts, 1999; Keene et al., 1999), nitric acid anhydride, N_2O_5 (McLaren et al., 2004) and organic acids (Laskin et al., 2012). The displacement by HNO_3 and H_2SO_4 is particularly important during the daytime, since it involves the photo-oxidation of nitrogen and sulfur oxides respectively. At night, however, N_2O_5 ,
20 formed from the reaction of NO_2 and NO_3 , can contribute significantly to acid displacement and subsequent formation of HCl. Some of the HCl can repartition into the aerosol through reaction with ammonia and/or dissolve in hygroscopic aerosols directly in environments with high water content, such as marine environments, especially if the aerosols are non-acidic in nature (Keene et al., 1999; Kim et al., 2008).

Separating refractory and non-refractory particulate chloride

I. Nuaaman et al.

Title Page

Abstract

Introduction

Conclusions

References

Tables

Figures



Back

Close

Full Screen / Esc

Printer-friendly Version

Interactive Discussion



Separating refractory and non-refractory particulate chloride

I. Nuaaman et al.

Title Page

Abstract

Introduction

Conclusions

References

Tables

Figures



Back

Close

Full Screen / Esc

Printer-friendly Version

Interactive Discussion



The HCl released during acid displacement (Finlayson-Pitts and Pitts, 1999; and references therein) is a significant sink of ssCl (Keene et al., 1999). The released HCl can lead to halogen activation since HCl can react with the hydroxyl radical, OH, to form chlorine atoms in the gas phase. Other secondary sources of HCl include the reaction of chlorine atoms with methane and other VOCs (Kim et al., 2008; Mielke et al., 2011). Chlorine atoms are also formed from the photolysis of nitryl chloride, ClNO₂, and molecular chlorine, Cl₂ (Osthoff et al., 2008; Roberts et al., 2008; Riedel et al., 2012).

Aerosol mass spectrometry (AMS) has become a common method for continuous measurement of submicron aerosols (Canagaratna et al., 2007). The AMS used in this study contains a critical orifice and aerodynamic lens that allows sampling of submicron aerosols 70 to 700 nm (50 % vacuum aerodynamic cutoff diameter) in diameter at 1×10^5 Pa (Liu et al., 2007). Sub-micron aerosols impact a heater in the AMS that is typically set at 600 °C, which is not high enough to efficiently vaporize refractory (*R*) aerosol components such as sea salt, many mineral oxides, elemental carbon (soot) and metals. For this reason, the AMS is not expected to measure refractory sea salt aerosols in a quantitative way whereas, most non-refractory (NR) aerosol species, such as organics and many inorganic salts (i.e.: NH₄Cl, NH₄NO₃ and (NH₄)₂SO₄) are efficiently vaporized and ionized upon impact by an electron beam, with subsequent detection in the mass spectrometer.

Given these operational conditions, one would assume that literature reported aerosol mass loadings of submicron chloride, via the AMS, would only contain non-refractory chloride and that refractory components such as NaCl should be absent since NaCl has a melting point of 800.7 °C and a boiling point of 1465 °C (Haynes, 2012), much higher than the vaporizer temperature of 600 °C. However in coastal environments, where there are both sea spray and non-sea spray sources of pCl, uncertainties exist in terms of exactly what is being reported since the vaporization of sea salt NaCl is not zero at 600 °C. In fact, NaCl signals using a HR-AMS have been observed in the South Atlantic marine boundary layer and found to correlate positively with wind

speed, a surrogate for wave action (Zorn et al., 2008). More recently, total sea salt concentration in the submicron range was quantified using an HR-AMS by utilizing the $\text{Na}^{35}\text{Cl}^+$ ion signal as a sea salt surrogate (Ovadnevaite et al., 2012). Neither study, however, quantified ssCl.

This paper reports measurements of aerosol chloride using the HR-AMS deployed onboard the research vessel *Atlantis* during the CalNex study in 2010 (Ryerson et al., 2013). The CalNex campaign goal was to measure ambient aerosol concentrations, composition and microphysical properties along the coast of California (Cappa et al., 2012; Massoli et al., 2014). In addition, nascent sea spray aerosols were artificially generated through in situ bubbling of seawater during sea sweep experiments (Bates et al., 2012), and sampled by the HR-AMS. We detected high levels of refractory NaCl in the sea sweep aerosols, as well as in the ambient marine environment throughout the study.

This work seeks to provide clarity on the reporting of particulate chloride using AMS instruments. In particular, we propose a way to correct pCl signals for the presence of ssCl signals that can be abundant in areas impacted by sea salt aerosol, such that the more volatile non sea salt chloride (nssCl) can be reported more accurately. This study also proposes a method to establish the percentage of ssCl that is depleted from sea salt aerosols. Both methods utilize the $\text{Na}^{35}\text{Cl}^+$ ion signal, but the latter method also utilizes the Na^+ ion signal. Finally, a method to establish total submicron chloride concentrations is presented. Submicron chloride concentrations are established strictly from HR-AMS data and account for both ssCl and nssCl.

2 Experimental

The HR-AMS (Aerodyne Research Inc., Billerica, MA, USA) was deployed onboard the R/V *Atlantis* for the measurements of submicron aerosol concentration and composition. The R/V *Atlantis* departed San Diego on 14 May 2010 and made its way north along the Pacific coast to Los Angeles and Long Beach areas; then north along the

Separating refractory and non-refractory particulate chloride

I. Nuaaman et al.

Title Page

Abstract

Introduction

Conclusions

References

Tables

Figures



Back

Close

Full Screen / Esc

Printer-friendly Version

Interactive Discussion



coast towards San Francisco and east towards Sacramento through the deep water-
shipping channel, returning to the Port of San Francisco on 8 June 2010. Aerosols
were sampled from a 6 m mast that was 18 m above the sea surface and forward of
the ship's stack. A submicron impactor with a 1.1 μm cutoff was placed upstream of
the HR-AMS and the relative humidity was maintained at about 55 % in the inlet (Bates
et al., 2012; Cappa et al., 2012).

A detailed description of the HR-AMS has been given elsewhere (DeCarlo et al.,
2006; Canagaratna et al., 2007). Briefly, air is sampled through a critical orifice then
an aerodynamic lens, which focuses aerosol particles in the 70 to 700 nm size range
(50 % cutoff) at 1×10^5 Pa (Liu et al., 2007). After the particles have been focused into
a narrow beam, supersonic expansion at 10^{-5} Torr accelerates the particles into the
particle time-of-flight (pToF) sizing region, initiated with a beam chopper, and subse-
quently into the vaporization region. Particles are flash vaporized at the end of the
sizing region on a resistively heated surface held at 600 °C. The vapor is then ion-
ized by electron impact at 70 eV. The ions are perpendicularly extracted into a high-
resolution time of flight mass spectrometer, which can operate either in the V-mode
(lower resolution, high sensitivity) or the W-mode (high resolution, lower sensitivity). In
this study, the AMS alternated between the V-mode and W-mode in a 2.5 min cycle.
In the V-mode the sampling was evenly split between the mass spectrum (MS) mode
and the particle time of flight (pToF) mode. A collection efficiency (CE) of 0.47 was
determined for the non-refractory aerosol components based upon a comparison of
the data with aerosol filter measurements coupled with ion chromatography (IC) anal-
ysis and measurements made using a quadrupole AMS. As such, a correction factor
of 2.1 was applied to the data set (1/CE). This factor corrects for loss of particles in
the inlet and the particle bounce at the vaporizer upon impact. The CE correction also
accounts for transmission losses of aerosols when sampling off the aerosol mast. The
derived CE is consistent with a value of 0.5 that is commonly observed and used for the
AMS (Canagaratna et al., 2007). Data analysis was performed using the SQUIRREL
(v1.51C) and PIKA (v1.10C) software packages (D. Sueper, 2010, <http://cires.colorado>).

Separating refractory and non-refractory particulate chloride

I. Nuaaman et al.

Title Page

Abstract

Introduction

Conclusions

References

Tables

Figures



Back

Close

Full Screen / Esc

Printer-friendly Version

Interactive Discussion



edu/jimenez-group/ToFAMSResources/ToFSoftware/index.html). In this study we only report data collected in the V-mode. All data were averaged to 10 min to improve the signal to noise ratio, unless otherwise stated. Using the AMS, aerosol mass concentrations (C) for a species X is determined using the following equation (Jimenez et al., 2003; Canagaratna et al., 2007):

$$C = \frac{MW_{NO_3}}{RIE_x IE_{NO_3} Q N_A} \sum_i I_{x,i} \quad (1)$$

where MW is the molecular weight of the species, Q is sampling flow rate, N_A is Avogadro's number and IE is the ionization efficiency, a dimensionless quantity that measures the ionization and detection efficiency and is defined as the ratio of the ions detected to the parent molecules vaporized. The IE_{NO_3} was established through calibrations using monodispersed 300 nm diameter NH_4NO_3 particles during the study. RIE_x is the relative ionization efficiency of X relative to that of NO_3^- (Alfarra, 2004). $I_{x,i}$ refers to the ion count rate (in Hz) of ion fragment i that results from the ionization of X . When the RIE of X is not known nor utilized in Eq. (1), the value obtained is referred to as the nitrate equivalent concentration (NEC) (Jimenez et al., 2003; Canagaratna et al., 2007), a proxy of signal intensity. For chloride, a RIE of 1.3 is commonly used (e.g. Lee et al., 2013; McGuire et al., 2014), based on the methodology by Jimenez et al. (2003) and Alfarra et al. (2004). In this study, we introduce and utilize the chloride equivalent concentration (CEC), a surrogate for measured mass loadings that utilizes a RIE of 1.3. This will be used for some species with unknown RIE values such as NaCl. Finally, we define an ion group H_xCl^+ , which is the sum of ions typically used to establish the AMS chloride signal. H_xCl^+ includes ion signals at m/z 34.97 ($^{35}Cl^+$), 35.97 ($H^{35}Cl^+$), 36.97 ($^{37}Cl^+$) and 37.97 ($H^{37}Cl^+$), where the contributions of $^{37}Cl^+$ and $H^{37}Cl^+$ are estimated using chlorine isotopic ratios (Allan et al., 2004).

Ambient submicron aerosol (50 % aerodynamic cut-off diameter, D_a , < 1.1 μm at 60 % RH) was also sampled using one and two-stage multijet cascade impactors (Berner et al., 1979). The ambient mass concentrations of Na^+ , Cl^- (henceforth $[Na^+]$

Separating refractory and non-refractory particulate chloride

I. Nuaaman et al.

Title Page

Abstract

Introduction

Conclusions

References

Tables

Figures



Back

Close

Full Screen / Esc

Printer-friendly Version

Interactive Discussion



and $[Cl^-]$) and other ions on the filters used in the impactor were determined using Ion Chromatography (IC) (Quinn et al., 1998). The time resolution of these filter measurements was 2–16 h with a frequency of 1–3 per day.

In addition to ambient air aerosol measurements, Sea Sweep experiments were conducted periodically while at sea during the CalNex 2010 study to measure artificially generated nascent sea spray aerosols (Bates et al., 2012). Briefly, a Sea Sweep experiment was performed by bubbling clean air just below the ocean surface, while instruments sampled the sea salt aerosols created by bubble bursting above the surface in an enclosure. Ambient particles are prevented from entering the Sea Sweep enclosure with a curtain of particle-free air surrounding the enclosure. Hence, only freshly emitted sea spray aerosols, not modified by mixing or reaction with ambient particles, are sampled. The Sea Sweep setup was positioned off the port bow while the ship position blocked the true wind. When sampling, the ship steamed slowly at 0.2 m s^{-1} to ensure continuous renewal of sampled sea surface. Data from seven Sea Sweep experiments (0.6–5 h length) are included in the present analysis.

3 Results and discussion

3.1 Mass spectrum of sea salt aerosols

An average aerosol mass spectrum obtained using the HR-AMS for the Sea Sweep experiments is shown in Fig. 1. The mass spectrum includes the ions for aerosol species typically measured and reported by the AMS including particulate organics (OM), sulfate (SO_4), ammonium (NH_4) and nitrate (NO_3). Figure 1 also shows the H_xCl^+ ion group, which is typically utilized to determine chloride concentration using an AMS. Also included in the mass spectrum are ions observed that are typical of sea salt aerosol components namely, Na^+ , $NaCl^+$, Mg^+ , $MgCl^+$, K^+ and KCl^+ . Other ion signals (such as metal ions) were grouped under the “Other” category, while air and water signals were not included for clarity.

Separating refractory and non-refractory particulate chloride

I. Nuaaman et al.

Title Page

Abstract

Introduction

Conclusions

References

Tables

Figures



Back

Close

Full Screen / Esc

Printer-friendly Version

Interactive Discussion



Separating refractory and non-refractory particulate chloride

I. Nuaaman et al.

Title Page

Abstract

Introduction

Conclusions

References

Tables

Figures



Back

Close

Full Screen / Esc

Printer-friendly Version

Interactive Discussion



The most dominant ion signals in Fig. 1, in order of intensity are: Na^+ at m/z 22.99, particulate organic material (pOM) components such as m/z 43.99 (CO_2^+) and 41.04 (C_3H_5^+), H_xCl^+ components at m/z 34.97 ($^{35}\text{Cl}^+$), 35.97 (H^{35}Cl^+), 36.97 ($^{37}\text{Cl}^+$) and 37.97 (H^{37}Cl^+), SO_4 components such as m/z 47.97 (SO^+) and 63.96 (SO_2^+), as well as $\text{Na}^{35}\text{Cl}^+$ at m/z 57.96 and $\text{Na}^{37}\text{Cl}^+$ at m/z 59.96. The $\text{Na}^{37}\text{Cl}^+$ to $\text{Na}^{35}\text{Cl}^+$ ratio is 0.32 : 1, in agreement with chlorine's natural isotopic abundances (Numata et al., 2001). The OM signals result from biogenic derived organic matter that is injected into the marine aerosol during bubble bursting (Bates et al., 2012). The dominance of ion signals associated with sodium chloride (i.e., Na^+ , H_xCl^+ and NaCl^+ ions) during the sea sweep experiments was similar to that observed by Ovadnevaite et al. (2012) during sampling of ambient marine aerosols. Even though sodium chloride is not efficiently detected by the AMS operating with a 600 °C vaporizer temperature, large ion signals are still apparent in the mass spectrum given the large amounts of sea salt sampled during these experiments. Even if only a small fraction of NaCl is vaporized, ionized and detected, this fraction appears dominant in the mass spectrum for the sea sweep experiments. It is worth noting that the standard AMS data analysis reports total aerosol chloride (pCl) using the H_xCl^+ mass fragments outlined above, but does not include the NaCl^+ ions, as NaCl is assumed to be truly refractory. In default AMS applications, it is also assumed that aerosol chloride species are evaporated with unit efficiency. It should be obvious from the sea sweep signals in Fig. 1 that any report of non-refractory chloride mass (nssCl) in areas that contain sea salt aerosols (such as coastal areas) will be compromised, largely due to the vast difference in vaporization efficiency of refractory and non refractory seasalt aerosols. Under those conditions when sea salt contributes to the H_xCl^+ signal, aerosol chloride (pCl) reported using standard assumptions will underestimate sea salt chloride and overestimate the non-refractory chloride component.

3.2 Observation of sea salt chloride (ssCl) in ambient air

During the study, the Na^+ , $\text{Na}^{35}\text{Cl}^+$ and $\text{Na}^{37}\text{Cl}^+$ signals were low but detectable with well-resolved peaks indicating that sea salt was sampled and detected by the AMS. The $\text{Na}^{37}\text{Cl}^+$ peak at 59.956, however, has significant overlaps with potential interfering ions, CSO^+ (59.967) and SiO_2^+ (59.967), even at the high resolution of this AMS, and was thus not used as a quantitative indicator of sea salt. Figure 2 shows a time series of H_xCl^+ , Na^+ and $\text{Na}^{35}\text{Cl}^+$ signals throughout CalNex including ambient air measurements and sea sweep experiments. The highest H_xCl^+ signals observed during sea sweep experiments reached $2 \mu\text{g m}^{-3}$, undoubtedly due to the sampling of NaCl in sea salt during these experiments. The coincident Na^+ and NaCl^+ signals correlate strongly with the H_xCl^+ signal during these experiments, peaking at 1.8 and $0.41 \mu\text{g m}^{-3}$ respectively. Note that these chloride equivalent concentrations should only be treated as relative signals and not true concentrations.

The NaCl signal was characterized by slow evaporation in the AMS after sampling high sea salt aerosol during the sea sweep experiments. This slow evaporation led to high background signal for certain ions, which was apparent from the chopper “closed” signal. In the AMS, the beam chopper alternates between blocking position, (closed) and transmitting position (open) of the aerosol beam. The aerosol signature is then properly quantified by subtracting the chopper-closed signal from the chopper-open signal). During this study, the background signals for Na^+ , H_xCl^+ and $\text{Na}^{35}\text{Cl}^+$ were much higher than the “open – closed” measurement signal after sea sweep experiments. Similar trends were observed in other studies for sodium and lead signals when using an AMS for sampling refractory aerosols (Salcedo et al., 2010; Ovadnevaite et al., 2012). In this study, we found that the time for complete disappearance of refractory sea salt signals was directly proportional to the amount of sea salt sampled and ranged from 5 to 28 h for Na^+ , 2.2 to 6.8 h for H_xCl^+ and 0.07 to 5.2 h for $\text{Na}^{35}\text{Cl}^+$. Ovadnevaite et al. (2012) reported the time for complete refractory signal disappearance to be about 12 h for Na^+ , 2 h for H_xCl^+ and < 0.083 h for $\text{Na}^{35}\text{Cl}^+$, all of which compare well with

Separating refractory and non-refractory particulate chloride

I. Nuaaman et al.

Title Page

Abstract

Introduction

Conclusions

References

Tables

Figures



Back

Close

Full Screen / Esc

Printer-friendly Version

Interactive Discussion



our observations. This high background signal resulted in a low signal to noise ratio for the ambient measurements that followed the sea sweep experiments; and so we have eliminated these time periods from further analysis. The difference in background signal recovery times for the different components of the same parent compound is not fully understood.

The observation of Na^+ and NaCl^+ signals in ambient aerosol measurements confirms the detection of refractory sodium chloride by the AMS. Thus, refractory chloride contributes to the H_xCl^+ ion family, which is typically used to calculate non-refractory chloride (i.e., nssCl in the form of HCl, NH_4Cl or other volatile chlorinated species) mass concentrations via the AMS. It then follows that the contribution of this refractory component to the H_xCl^+ signal needs to be corrected before reporting mass concentrations of nssCl. To do this, it is necessary to isolate the nssCl signal from the H_xCl^+ signal. In the following section, we present a method to establish nssCl concentration from H_xCl^+ and $\text{Na}^{35}\text{Cl}^+$ signals.

3.3 A method to establish nssCl with sea salt chloride interferences

In order to correctly report nssCl we need to estimate the refractory component of H_xCl^+ , which we define to be the chloride portion of the H_xCl^+ signal that is in the form of NaCl. For this estimate, we use an ion (I) that is not a part of the H_xCl^+ group that results exclusively from the fragmentation and ionization of NaCl. In addition, we establish the $\text{H}_x\text{Cl}^+//I$ ratio for NaCl in sea salt aerosol using the HR-AMS. For I , one can consider using Na^+ or $\text{Na}^{35}\text{Cl}^+$, but while $\text{Na}^{35}\text{Cl}^+$ is expected to result exclusively from the ionization of NaCl, Na^+ could also additionally arise from chloride depleted sea salt aerosol in the form of NaNO_3 and/or Na_2SO_4 . This is especially true with aged sea salt aerosols, where acid displacement can remove chloride (see Finlayson-Pitts and Pitts, 1999, and references therein). It is therefore advantageous to use the $\text{Na}^{35}\text{Cl}^+$ signal to correct for the refractory component of H_xCl^+ , since this signal only arises from NaCl in sea salt aerosols. The ratio $\text{H}_x\text{Cl}^+/\text{Na}^{35}\text{Cl}^+$ for sea salt chloride from NaCl in this work is established using sea sweep experiments.

Separating refractory and non-refractory particulate chloride

I. Nuaaman et al.

Title Page

Abstract

Introduction

Conclusions

References

Tables

Figures



Back

Close

Full Screen / Esc

Printer-friendly Version

Interactive Discussion



to $\text{Na}^{35}\text{Cl}^+$ ratio higher than the confidence interval line are expected to have additional contributions to the H_xCl^+ signal from nssCl. We note that most of the ambient data (pink points) fall above the upper confidence line indicating significant contributions of the H_xCl^+ signal from aerosols containing non-refractory chloride. However, Fig. 4 also shows that such data also has contributions to the H_xCl^+ signal from ssCl proportional to the $\text{Na}^{35}\text{Cl}^+$ signal that should be subtracted if one wishes to report nssCl alone. In order to establish the concentration of nssCl, we use the following equation that utilizes the H_xCl^+ to $\text{Na}^{35}\text{Cl}^+$ ratio from sea sweep experiments and the H_xCl^+ and $\text{Na}^{35}\text{Cl}^+$ ionic signals:

$$\text{nssCl} (\mu\text{g m}^{-3}) = \text{H}_x\text{Cl}^+ - 3.9 \times \text{Na}^{35}\text{Cl}^+ \quad (3)$$

where the term in parentheses refers to the refractory Cl component of the ambient H_xCl^+ signal. Note that for the above equation, the intercept was forced to zero and only the H_xCl^+ to $\text{Na}^{35}\text{Cl}^+$ ratio was used. A zero intercept is within error and both the H_xCl^+ and $\text{Na}^{35}\text{Cl}^+$ signals are from the same source in sea sweep experiments (correlation is improved with a forced zero intercept, $R^2 = 0.95$). Using the last term in Eq. (2), we can quantify the contribution of refractory H_xCl^+ to the total H_xCl^+ signal, i.e. how much of the H_xCl^+ signal can be attributed to NaCl. This contribution is estimated by $(3.9 \times \text{Na}^{35}\text{Cl}^+)/\text{H}_x\text{Cl}^+ \times 100\%$, and the result of this estimation is shown in Fig. 5. Also shown in Fig. 5 is the submicron chloride concentration from filter measurements, which primarily detects NaCl, but not nssCl, due to evaporation issues of volatile chlorinated compounds (such as NH_4Cl) from the filters. The contribution of refractory H_xCl^+ to the total H_xCl^+ signal is reasonably correlated with $[\text{Cl}^-]$ measured with filters and captures the time trends well, suggesting high contributions of refractory H_xCl^+ to the total H_xCl^+ signal during periods of elevated ssCl concentrations.

Using the $\text{Na}^{35}\text{Cl}^+$ ion fragment and the factor of 3.9, the refractory H_xCl^+ signal detected by the HR-AMS was low in ambient air during this study. However, the contribution of refractory H_xCl^+ to the total H_xCl^+ signal in ambient air (not sea sweeps) was

Separating refractory and non-refractory particulate chloride

I. Nuaaman et al.

Title Page

Abstract

Introduction

Conclusions

References

Tables

Figures



Back

Close

Full Screen / Esc

Printer-friendly Version

Interactive Discussion



significant with a maximum contribution of 89 % and an average contribution of 10 %. In this study, periods with high refractory contributions to the H_xCl^+ signal were also periods of relatively low H_xCl^+ signals that were not enriched with nssCl.

3.4 A method to establish ssCl and pCl from AMS measurements

In this section we will propose an empirical formula to estimate the air concentrations of submicron sea salt chloride ssCl and total submicron ambient chloride pCl. In order to estimate ssCl, we use $NaCl^+$ and a scaling factor established using $[Cl^-]$ from filters. The ratio of submicron chloride from filters to $Na^{35}Cl^+$ (Fig. 3) was found to be 98.9 ± 6.7 , Sea salt chloride concentration is therefore estimated to be:

$$ssCl = 98.9 \times Na^{35}Cl^+ \quad (4)$$

assuming that all of the chloride measured on the filters is in the form of NaCl. This assumption is reasonable, since the filter measurements employed here do not detect volatile chlorinated species as mentioned previously. Now that we have a measure of nssCl and ssCl, pCl can be estimated using the following equation:

$$pCl(\mu g m^{-3}) = nssCl + 98.9 \times Na^{35}Cl^+ \quad (5)$$

where the first term is nssCl calculated using Eq. (3) and the second term is ssCl calculated using Eq. (4). Figure 6 shows the time series of pCl, nssCl and ssCl concentrations measured by the HR-AMS, as well as submicron $[Cl^-]$ from filters. The lack of sensitivity of the filter measurements to nssCl is apparent from Fig. 6 as an increase in nssCl does not coincide with an increase in $[Cl^-]$. In this study, the median levels (5, 95 percentiles) observed for pCl, nssCl and ssCl were $0.051, \mu g m^{-3}$ (0.012, 0.33), $0.017 \mu g m^{-3}$ (0.0096, 0.077) and $0.024 \mu g m^{-3}$ (0, 0.30) respectively. The average contributions of nssCl and ssCl to pCl were 48 and 52 % respectively. The nssCl dominated during periods of continental outflow (Massoli et al., 2014), while the ssCl dominated during periods when the air was not affected by urban air masses. The method proposed here for total submicron chloride determination has an advantage over filter

Separating refractory and non-refractory particulate chloride

I. Nuaaman et al.

Title Page

Abstract

Introduction

Conclusions

References

Tables

Figures



Back

Close

Full Screen / Esc

Printer-friendly Version

Interactive Discussion



measurements due to its high temporal resolution and since filter measurements may not be sensitive to semi-volatile NH_4Cl and other volatile chlorinated compounds, as seen in this study.

3.5 Estimating total sea salt concentrations from the $\text{Na}^{35}\text{Cl}^+$ signal

As discussed in Sect. 3.3, total submicron sea salt aerosol concentrations [sea salt] can be established from filter measurements and Eq. (2). The linear regression of [sea salt] from filter measurements to $\text{Na}^{35}\text{Cl}^+$ had a slope of 370 ± 19 and $R^2 = 0.89$ (Fig. 3), Ovadnevaite et al. (2012) used nitrate equivalent NaCl^+ concentration and a scaling factor of 51 to establish the concentration of submicron sea salt aerosol. The scaling factor proposed by Ovadnevaite would be equal to 66 (using chloride RIE of 1.3) if they had used $\text{Na}^{35}\text{Cl}^+$, which is 5.6 times lower than the scaling factor reported here. This difference could be attributed to the higher vaporizer temperature utilized by Ovadnevaite et al. (2012), 650°C , compared to 600°C used in this study. Figure 7 shows the sea salt concentrations determined from the HR-AMS $\text{Na}^{35}\text{Cl}^+$ signal and scaling factor of 370 as well as those determined from the filter measurements and Eq. (2). The two methods compare favorably. The average submicron sea salt concentration determined by the HR-AMS method was $0.28 \mu\text{g m}^{-3}$, with a maximum of $2.3 \mu\text{g m}^{-3}$ on 5/21. In comparison, the sea salt concentrations observed off the coast of Ireland by Ovadnevaite et al. (2012) were higher with a maximum of $4.5 \mu\text{g m}^{-3}$, likely attributable to the higher wind speeds experienced in their study compared to this study.

3.6 Determining chloride depletion in sea salt using AMS data

We now present a method to establish the percentage of chloride depleted from submicron sea salt in ambient air using HR-AMS ion signal measurements exclusively. Chloride depletion is an important indicator of sea salt aerosol aging and the formation of activated chloride in the form of HCl. Chloride depletion is typically calculated using the difference between the expected ssCl and observed ssCl (Zhao and Gao, 2008) as

Separating refractory and non-refractory particulate chloride

I. Nuaaman et al.

Title Page

Abstract

Introduction

Conclusions

References

Tables

Figures



Back

Close

Full Screen / Esc

Printer-friendly Version

Interactive Discussion



follows,

$$\% \text{ Cl depletion} = \frac{\text{expected ssCl} - \text{observed ssCl}}{\text{expected ssCl}} \times 100\% = \frac{1.81[\text{Na}^+] - [\text{Cl}^-]}{1.81[\text{Na}^+]} \times 100\% \quad (6)$$

The expected ssCl in Eq. (6) is estimated from the sodium concentration and mass ratio of Cl^- to Na^+ in seawater, $1.81 \mu\text{g m}^{-3} (\mu\text{g m}^{-3})^{-1}$ (Haynes, 2012). The estimation assumes that sodium remains in the aerosol phase when chloride is volatilized by acid displacement reactions.

The expected ssCl signal from the AMS can be estimated using the Na^+ signal and the $\text{H}_x\text{Cl}^+/\text{Na}^+$ ratio derived from the sea sweep experiments, while the observed ssCl signal is estimated as $3.9 \times \text{Na}^{35}\text{Cl}^+$ as discussed in Sect. 3.3. Figure 8 is a plot of H_xCl^+ signal vs. Na^+ signal for Sea Sweep experiments. The Na^+ signal is well correlated with H_xCl^+ ($R^2 = 0.94$) and a $\text{H}_x\text{Cl}^+/\text{Na}^+$ ratio of $0.827 \pm 0.018 \mu\text{g m}^{-3} (\mu\text{g m}^{-3})^{-1}$. Note that this ratio should be viewed as a signal ratio, since chloride equivalent concentrations are used as ion signals in this study. As such, the above ratio cannot be directly compared to the true $[\text{Cl}^-]$ to $[\text{Na}^+]$ ratio of 1.81. The difference between the two ratios is due to different ionization efficiencies in the HR-AMS for chloride and sodium. Using the aforementioned estimates for expected and observed chloride, the HR-AMS estimate of submicron sea salt chlorine depletion can be written:

$$\% \text{ Cl depletion} = \frac{0.827 \times \text{Na}^+ - 3.9 \times \text{Na}^{35}\text{Cl}^+}{0.827 \times \text{Na}^+} \quad (7)$$

Figure 9 shows the time series of the percentage chloride depletion in submicron aerosols during the CalNex study for both ambient aerosols and sea sweep experiments. For ambient air, the percentage chloride depletion was calculated using two methods. The first uses the HR-AMS measurements and Eq. (7). The second method uses the filter measurements and Eq. (6). The HR-AMS method was exclusively used

Separating refractory and non-refractory particulate chloride

I. Nuaaman et al.

Title Page

Abstract

Introduction

Conclusions

References

Tables

Figures



Back

Close

Full Screen / Esc

Printer-friendly Version

Interactive Discussion



to establish chloride depletions using sea sweep experiments, since filters were not available for these experiments. Hourly averages of the HR-AMS data were used to reduce noise in the Na^+ signals. From Fig. 9, the chloride depletion during the sea sweep experiments was very close to zero, which is expected since fresh sea salt aerosols were sampled during these experiments and the ratios used in Eq. (7) were derived from these experiments. For ambient data, the HR-AMS method gives reasonable results with $\sim 95\%$ of the data in the 0–100% range, $\sim 5\%$ are less than zero and are attributed to the noise associated with the HR-AMS. Both methods show similar trends (Fig. 9) and are positively correlated, which provides confidence to the method proposed here. The HR-AMS method captures more variations due to the higher time resolution of the measurements. The median chloride depletion observed in this study (HR-AMS method) was 78% with 5 and 95 percentiles of 0 and 96%. It is important to note that the method proposed here only considers chloride depletion from NaCl and does not take into account other chlorinated species in sampled aerosols.

4 Conclusions

This study attempts to provide some clarity and presents new methods in the reporting of aerosol chloride with the aerosol mass spectrometer. The issue that arises in the interpretation of different AMS datasets is that the chloride signal, typically measured via the H_xCl^+ ion group, has contributions from both non-refractory (i.e., NH_4Cl , HCl, organic chlorides, etc.) and refractory chloride species (i.e., NaCl) albeit with vastly different sensitivities. The AMS is a couple orders of magnitude less sensitive to the detection of refractory sea salt chloride (ie. ssCl) compared to non-refractory chloride at typical operational heater temperatures (600°C) due to the high boiling point of NaCl. However, the atmospheric loading of ssCl can be much higher than non sea salt chloride (nssCl) in environments conducive to the production of sea salt aerosol. To properly report submicron aerosol chloride in such environments, one needs to know what fraction of the H_xCl^+ ion group signal arises from the two different types of compo-

Separating refractory and non-refractory particulate chloride

I. Nuaaman et al.

Title Page

Abstract

Introduction

Conclusions

References

Tables

Figures



Back

Close

Full Screen / Esc

Printer-friendly Version

Interactive Discussion



nents. In this study we use the $\text{Na}^{35}\text{Cl}^+$ ion signal as the tracer for detection of ssCl to help us separate the two signal components and to report separately nssCl and ssCl, as well as total chloride (pCl), which is the sum of nssCl and ssCl.

We used data from sea sweep experiments when it was known that aerosols being sampled were 100% sea salt, to calibrate the $\text{H}_x\text{Cl}^+/\text{Na}^{35}\text{Cl}^+$ signal ratio (3.9 ± 0.2) for our operational conditions. The nssCl is then obtained by subtraction of the sea salt portion of the H_xCl^+ signal (Eq. 3). During ambient aerosol measurements in this study, we found that the sea salt chloride contribution to the H_xCl^+ signal averaged $\sim 10\%$, with a maximum of $\sim 90\%$. The contribution is expected to be even higher in marine areas with stronger wave breaking and in areas where nssCl levels are low. The ssCl (Eq. 4) was obtained via calibrations of the $[\text{Cl}]_{\text{filter}}/\text{Na}^{35}\text{Cl}^+$ ratio (98.9 ± 6.7) from ambient measurements with the assumption that the filter measurements are not sensitive to non refractory chloride (i.e. NH_4Cl), which evaporates from the filters. The true submicron total chloride is then obtained by adding ssCl and nssCl (Eq. 5). The two ratios referred to above that were established in this study are more than likely, highly dependent on AMS operating conditions and should be calibrated with individual instruments and conditions. In particular, small changes in the AMS heater temperature, either through changing the filament current or due to instrument temperature drift, are known to result in large changes in the evaporation efficiency of refractory sea salt components. Regular calibrations of these ratios should be part of future applications.

Similar to the determination of ssCl, we estimated the total sea salt aerosol concentration in ambient air by multiplying the sea salt surrogate signal, $\text{Na}^{35}\text{Cl}^+$, by the calibrated $[\text{seasalt}]/\text{Na}^{35}\text{Cl}^+$ ratio (370 ± 19) determined via co-sampled filters and HR-AMS measurements. Total submicron sea salt concentrations had a maximum of $2.3 \mu\text{g m}^{-3}$ during this study. We caution again that the ratio used to determine sea salt concentrations is highly dependent on instrument conditions and should be calibrated regularly.

Separating refractory and non-refractory particulate chloride

I. Nuaaman et al.

Title Page

Abstract

Introduction

Conclusions

References

Tables

Figures



Back

Close

Full Screen / Esc

Printer-friendly Version

Interactive Discussion



Separating refractory and non-refractory particulate chloride

I. Nuaaman et al.

[Title Page](#)[Abstract](#)[Introduction](#)[Conclusions](#)[References](#)[Tables](#)[Figures](#)[Back](#)[Close](#)[Full Screen / Esc](#)[Printer-friendly Version](#)[Interactive Discussion](#)

Finally, this study proposes a method to establish the relative amount of chloride depletion from NaCl in ambient sea salt aerosol. This method strictly uses HR-AMS measurements and utilizes H_xCl^+/Na^+ and $H_xCl^+/Na^{35}Cl^+$ ratios in sea salt aerosols established from the sea sweep experiments. Using this method, the percentage depletion of chloride in submicron sea salt aerosols was observed to vary between 0–100 % for 95 % of the data, with outliers existing due to instrumental noise. The median submicron sea salt aerosol chloride depletion during the whole study was found to be quite high, 78 %. This is likely attributable to the fact that the measurements during CalNex were taken in California coastal polluted regions characterized by high NO_x sources and frequent land breeze outflow events.

Acknowledgements. This work was supported by Environment Canada's Clean Air Regulatory Agenda (CARA) and the Natural Sciences and Engineering Research Council of Canada. This work was funded in part by the NOAA Global Climate Project Office (# NA09AR4310125), the NOAA Health of the Atmosphere Program and the California Air Resources Board (CARB). The authors thank the crew of the R/V *Atlantis*, and Derek Coffman and Drew Hamilton of NOAA PMEL for their assistance and help during the project.

References

- Aiken, A. C., DeCarlo, P. F., Kroll, J. H., Worsnop, D. R., Huffman, J. A., Docherty, K. S., Ulbrich, I. M., Mohr, C., Kimmel, J. R., Sueper, D., Sun, Y., Zhang, Q., Trimborn, A., Northway, M., Ziemann, P. J., Canagaratna, M. R., Onasch, T. B., Alfarra, M. R., Prevot, A. S. H., Dommen, J., Duplissy, J., Metzger, A., Baltensperger, U., and Jimenez, J. L.: O/C and OM/OC ratios of primary, secondary, and ambient organic aerosols with high-resolution time-of-flight aerosol mass spectrometry, *Environ. Sci. Technol.*, 42, 4478–4485, 2008.
- Alfarra, M. R.: Insights into atmospheric organic aerosols using an aerosol mass spectrometer, Ph.D. Dissertation, University of Manchester, Manchester, 2004.
- Alfarra, M. R., Coe, H., Allan, J. D., Bower, K. N., Boudries, H., Canagaratna, M. R., Jimenez, J. L., Jayne, J. T., Garforth, A. A., Li, S.-M., and Worsnop, D. R.: Characterization of urban and rural organic particulate in the Lower Fraser Valley using two Aerodyne Aerosol Mass Spectrometers, *Atmos. Environ.*, 38, 5745–5758, 2004.

Separating refractory and non-refractory particulate chloride

I. Nuaaman et al.

Title Page

Abstract

Introduction

Conclusions

References

Tables

Figures



Back

Close

Full Screen / Esc

Printer-friendly Version

Interactive Discussion



Allan, J. D., Delia, A. E., Coe, H., Bower, K. N., Alfarra, M. R., Jimenez, J. L., Middlebrook, A. M., Drewnick, F., Onasch, T. B., Canagaratna, M. R., Jayne, J. T., and Worsnop, D. R.: A generalised method for the extraction of chemically resolved mass spectra from Aerodyne aerosol mass spectrometer data, *J. Aerosol Sci.*, 35, 909–922, 2004.

5 Andreae, M. O., Atlas, E., Harris, G. W., Helas, G., De, K., A, Koppmann, R., Maenhaut, W., Mano, S., Pollock, W. H., Rudolph, J., Scharffe, D., Schebeske, G., and Welling, M.: Methyl halide emissions from savanna fires in southern Africa, *J. Geophys. Res.*, 101, 23603–23613, doi:10.1029/95JD01733, 1996.

Bates, T. S., Quinn, P. K., Frossard, A. A., Russell, L. M., Hakala, J., T., P., Kulmala, M.,
10 Covert, D. S., Cappa, C. D., Li, S.-M., Hayden, K. L., Nuaaman, I., McLaren, R., Massoli, P., Canagaratna, M. R., Onasch, T. B., Sueper, D., Worsnop, D. R., and Keene, W. C.: Measurements of ocean derived aerosol off the coast of California, *J. Geophys. Res.*, 117, D00V15, doi:10.1029/2012JD017588, 2012.

Berner, A., Lurzer, C., Pohl, F., Preining, O., and Wagner, P.: The size distribution of the urban aerosol in Vienna, *Sci. Total Environ.*, 13, 245–261, 1979.

15 Cai, X. and Griffin, R. J.: Secondary aerosol formation from the oxidation of biogenic hydrocarbons by chlorine atoms, *J. Geophys. Res.*, 111, D14206, doi:10.1029/2005JD006857, 2006.

Canagaratna, M. R., Jayne, J. T., Jimenez, J. L., Allan, J. D., Alfarra, M. R., Zhang, Q.,
20 Onasch, T. B., Drewnick, F., Coe, H., Middlebrook, A., Delia, A., Williams, L. R., Trimborn, A. M., Northway, M. J., DeCarlo, P. F., Kolb, C. E., Davidovits, P., and Worsnop, D. R.: Chemical and microphysical characterization of ambient aerosols with the aerodyne aerosol mass spectrometer, *Mass Spectrom. Rev.*, 26, 185–222, 2007.

Cappa, C. D., Onasch, T. B., Massoli, P., Worsnop, D. R., Bates, T. S., Cross, E. S., Davidovits, P., Hakala, J., Hayden, K. L., Jobson, B. T., Kolesar, K. R., Lack, D. A., Lerner, B. M.,
25 Li, S. M., Mellon, D., Nuaaman, I., Olfert, J. S., Petaja, T., Quinn, P. K., Song, C., Subramanian, R., Williams, E. J., and Zaveri, R. A.: Radiative absorption enhancements due to the mixing state of atmospheric black carbon, *Science*, 337, 1078–1081, 2012.

DeCarlo, P. F., Kimmel, J. R., Trimborn, A., Northway, M. J., Jayne, J. T., Aiken, A. C., Gonin, M., Fuhrer, K., Horvath, T., Docherty, K. S., Worsnop, D. R., and Jimenez, J. L.:
30 Field-deployable, high-resolution, time-of-flight aerosol mass spectrometer, *Anal. Chem.*, 78, 8281–8289, 2006.

Separating refractory and non-refractory particulate chloride

I. Nuaaman et al.

[Title Page](#)[Abstract](#)[Introduction](#)[Conclusions](#)[References](#)[Tables](#)[Figures](#)[Back](#)[Close](#)[Full Screen / Esc](#)[Printer-friendly Version](#)[Interactive Discussion](#)

- Docherty, K. S., Stone, E. A., Ulbrich, I. M., DeCarlo, P. F., Snyder, D. C., Schauer, J. J., Peltier, R. E., Weber, R. J., Murphy, S. M., Seinfeld, J. H., Grover, B. D., Eatough, D. J., and Jimenez, J. L.: Apportionment of Primary and Secondary Organic Aerosols in Southern California during the 2005 Study of Organic Aerosols in Riverside (SOAR-1), *Environ. Sci. Technol.*, 42, 7655–7662, 2008.
- Finalyson-Pitts, B. J. and Pitts, J. N.: *Chemistry of the Upper and Lower Atmosphere: Theory, Experiments and Applications*, Academic Press, San Diego, 1999.
- Haynes, W. M.: *CRC Handbook of Chemistry and Physics*, CRC Press, Boca Raton, Florida, 2012.
- Hersey, S. P., Craven, J. S., Metcalf, A. R., Lin, J., Lathem, T., Suski, K. J., Cahill, J. F., Duong, H. T., Sorooshian, A., Jonsson, H. H., Shiraiwa, M., Zuend, A., Nenes, A., Prather, K. A., Flagan, R. C., and Seinfeld, J. H.: Composition and hygroscopicity of the Los Angeles Aerosol: CalNex, *J. Geophys. Res.-Atmos.*, 118, 3016–3036, 2013.
- Ianniello, A., Spataro, F., Esposito, G., Allegrini, I., Hu, M., and Zhu, T.: Chemical characteristics of inorganic ammonium salts in PM_{2.5} in the atmosphere of Beijing (China), *Atmos. Chem. Phys.*, 11, 10803–10822, doi:10.5194/acp-11-10803-2011, 2011.
- Jimenez, J. L., Jayne, J. T., Shi, Q., Kolb, C. E., Worsnop, D. R., Yourshaw, I., Seinfeld, J. H., Flagan, R. C., Zhang, X., Smith, K. A., Morris, J. W., and Davidovits, P.: Ambient aerosol sampling using the Aerodyne Aerosol Mass Spectrometer, *J. Geophys. Res.*, 108, 8425, doi:10.1029/2001JD001213, 2003.
- Keene, W. C., Khalil, M. A. K., Erickson, D. J., McCulloch, A., Graedel, T. E., Lobert, J. M., Aucott, M. L., Gong, S. L., Harper, D. B., Kleiman, G., Midgley, P., Moore, R. M., Seuzaret, C., Sturges, W. T., Benkovitz, C. M., Koropalov, V., Barrie, L. A., and Li, Y. F.: Composite global emissions of reactive chlorine from anthropogenic and natural sources: reactive Chlorine Emissions Inventory, *J. Geophys. Res.*, 104, 8429–8440, 1999.
- Kim, S., Huey, L. G., Stickel, R. E., Pierce, R. B., Chen, G., Avery, M. A., Dibb, J. E., Diskin, G. S., Sachse, G. W., McNaughton, C. S., Clarke, A. D., Anderson, B. E., and Blake, D. R.: Airborne measurements of HCl from the marine boundary layer to the lower stratosphere over the North Pacific Ocean during INTEX-B, *Atmos. Chem. Phys. Discuss.*, 8, 3563–3595, doi:10.5194/acpd-8-3563-2008, 2008.
- Laskin, A., Moffet, R. C., Gilles, M. K., Fast, J. D., Zaveri, R. A., Wang, B., Nigge, P., and Shutthanandan, J.: Tropospheric chemistry of internally mixed sea salt and organic parti-

Separating refractory and non-refractory particulate chloride

I. Nuaaman et al.

Title Page

Abstract

Introduction

Conclusions

References

Tables

Figures



Back

Close

Full Screen / Esc

Printer-friendly Version

Interactive Discussion



cles: surprising reactivity of NaCl with weak organic acids, *J. Geophys. Res.*, 117, D15302, doi:10.1029/2012JD017743, 2012.

Lee, B. P., Li, Y. J., Yu, J. Z., Louie, P. K. K., and Chan, C. K.: Physical and chemical characterization of ambient aerosol by HR-ToF-AMS at a suburban site in Hong Kong during springtime 2011, *J. Geophys. Res.-Atmos.*, 118, 8625–8639, 2013.

Lippmann, M., Ito, K., Nadas, A., and Burnett, R. T.: Association of particulate matter components with daily mortality and morbidity in urban populations, Research Report (Health Effects Institute) 95, 5–72, 2000.

Liu, P. S. K., Deng, R., Smith, K. A., Williams, L. R., Jayne, J. T., Canagaratna, M. R., Moore, K., Onasch, T. B., Worsnop, D. R., and Deshler, T.: Transmission efficiency of an aerodynamic focusing lens system: comparison of model calculations and laboratory measurements for the aerodyne aerosol mass spectrometer, *Aerosol Sci. Tech.*, 41, 721–733, 2007.

Livingston, C., Rieger, P., and Winer, A.: Ammonia emissions from a representative in-use fleet of light and medium-duty vehicles in the California South Coast Air Basin, *Atmos. Environ.*, 43, 3326–3333, 2009.

Massoli, P., Onasch, T. B., Cappa, C. D., Nuamaan, I., Hakala, J., Hayden, K., Li, S. M., Sueper, D. T., Bates, T. S., Quinn, P. K., Jayne, J. T., and Worsnop, D. R.: Characterization of black carbon-containing particles from soot particle aerosol mass spectrometer (SP-AMS) measurements on the R/V Atlantis during CalNex 2010, *J. Geophys. Res.*, submitted, 2014.

Matsumoto, K. and Tanaka, H.: Formation and dissociation of atmospheric particulate nitrate and chloride: an approach based on phase equilibrium, *Atmos. Environ.*, 30, 639–648, 1996.

McCulloch, A., Aucott, M. L., Benkovitz, C. M., Graedel, T. E., Kleiman, G., Midgley, P. M., and Li, Y.-F.: Global emissions of hydrogen chloride and chloromethane from coal combustion, incineration and industrial activities: Reactive Chlorine Emissions Inventory, *J. Geophys. Res.-Atmos.*, 104, 8391–8403, 1999.

McGuire, M. L., Chang, R. Y.-W., Slowik, J. G., Jeong, C.-H., Healy, R. M., Lu, G., Mihele, C., Abbatt, J. P. D., Brook, J. R., and Evans, G. J.: Enhancing non-refractory aerosol apportionment from an urban industrial site through receptor modeling of complete high time-resolution aerosol mass spectra, *Atmos. Chem. Phys.*, 14, 8017–8042, doi:10.5194/acp-14-8017-2014, 2014.

McLaren, R., Salmon, R. A., Liggio, J., Hayden, K. L., Anlauf, K. G., and Leaitch, W. R.: Night-time chemistry at a rural site in the Lower Fraser Valley, *Atmos. Environ.*, 38, 5837–5848, 2004.

Separating refractory and non-refractory particulate chloride

I. Nuaaman et al.

[Title Page](#)[Abstract](#)[Introduction](#)[Conclusions](#)[References](#)[Tables](#)[Figures](#)[Back](#)[Close](#)[Full Screen / Esc](#)[Printer-friendly Version](#)[Interactive Discussion](#)

- Mielke, L. H., Fergeson, A., and Osthoff, H. D.: Observation of CINO₂ in a mid-continental urban environment, *Environ. Sci. Technol.*, 45, 8889–8896, 2011.
- Neuman, J. A.: Variability in ammonium nitrate formation and nitric acid depletion with altitude and location over California, *J. Geophys. Res.*, 108, 4557, doi:10.1029/2003JD003616, 2003.
- Nowak, J. B., Neuman, J. A., Bahreini, R., Middlebrook, A. M., Holloway, J. S., McKeen, S. A., Parrish, D. D., Ryerson, T. B., and Trainer, M.: Ammonia sources in the California South Coast Air Basin and their impact on ammonium nitrate formation, *Geophys. Res. Lett.*, 39, L07804, doi:10.1029/2012GL051197, 2012.
- Numata, M., Nakamura, N., and Gamo, T.: Precise measurement of chlorine stable isotopic ratios by thermal ionization mass spectrometry, *Geochem. J.*, 35, 89–100, 2001.
- Osthoff, H. D., Roberts, J. M., Ravishankara, A. R., Williams, E. J., Lerner, B. M., Sommariva, R., Bates, T. S., Coffman, D., Quinn, P. K., Dibb, J. E., Stark, H., Burkholder, J. B., Talukdar, R. K., Meagher, J., Fehsenfeld, F. C., and Brown, S. S.: High levels of nitryl chloride in the polluted subtropical marine boundary layer, *Nature Geosci.*, 1, 324–328, 2008.
- OVadnevaite, J., Ceburnis, D., Canagaratna, M., Berresheim, H., Bialek, J., Martucci, G., Worsnop, D. R., and O'Dowd, C.: On the effect of wind speed on submicron sea salt mass concentrations and source fluxes, *J. Geophys. Res.*, 117, D16201, doi:10.1029/2011JD017379, 2012.
- Pio, C. A. and Harrison, R. M.: Vapour pressure of ammonium chloride aerosol: effect of temperature and humidity, *Atmos. Environ.*, 21, 2711–2715, 1987.
- Quinn, P. K., Coffman, D. J., Kapustin, V. N., Bates, T. S., and Covert, D. S.: Aerosol optical properties in the marine boundary layer during the First Aerosol Characterization Experiment (ACE 1) and the underlying chemical and physical aerosol properties, *J. Geophys. Res.*, 103, 16547–16563, 1998.
- Riedel, T. P., Bertram, T. H., Crisp, T. A., Williams, E. J., Lerner, B. M., Vlasenko, A., Li, S. M., Gilman, J., de Gouw, J., Bon, D. M., Wagner, N. L., Brown, S. S., and Thornton, J. A.: Nitryl chloride and molecular chlorine in the coastal marine boundary layer, *Environ. Sci. Technol.*, 46, 10463–10470, 2012.
- Roberts, J. M., Osthoff, H. D., Brown, S. S., and Ravishankara, A. R.: N₂O₅ oxidizes chloride to Cl₂ in acidic atmospheric aerosol, *Science*, 321, 1059–1059, 2008.
- Ryerson, T. B., Andrews, A. E., Angevine, W. M., Bates, T. S., Brock, C. A., Cairns, B., Cohen, R. C., Cooper, O. R., de, G., J. A., Fehsenfeld, F. C., Ferrare, R. A., Fischer, M. L.,

Separating refractory and non-refractory particulate chloride

I. Nuaaman et al.

Title Page

Abstract

Introduction

Conclusions

References

Tables

Figures



Back

Close

Full Screen / Esc

Printer-friendly Version

Interactive Discussion



Flagan, R. C., Goldstein, A. H., Hair, J. W., Hardesty, R. M., Hostetler, C. A., Jimenez, J. L., Langford, A. O., McCauley, E., McKeen, S. A., Molina, L. T., Nenes, A., Oltmans, S. J., Parrish, D. D., Pederson, J. R., Pierce, R. B., Prather, K., Quinn, P. K., Seinfeld, J. H., Senff, C. J., Sorooshian, A., Stutz, J., Surratt, J. D., Trainer, M., Volkamer, R., Williams, E. J., and Wofsy, S. C.: The 2010 California research at the Nexus of air quality and climate change (CalNex) field study, *J. Geophys. Res.-Atmos.*, 118, 5830–5866, doi:10.1002/jgrd.50331, 2013.

Salcedo, D., Onasch, T. B., Aiken, A. C., Williams, L. R., de Foy, B., Cubison, M. J., Worsnop, D. R., Molina, L. T., and Jimenez, J. L.: Determination of particulate lead using aerosol mass spectrometry: MILAGRO/MCMA-2006 observations, *Atmos. Chem. Phys.*, 10, 5371–5389, doi:10.5194/acp-10-5371-2010, 2010.

Solomon, S., Qin, D., Manning, M., Chen, Z., Marquis, M., Averyt, K. B., Tignor, M., and Miller, H. L.: IPCC, 2007: Climate Change 2007: The Physical Science Basis. Contribution of Working Group I to the Fourth Assessment Report of the Intergovernmental Panel on Climate Change Cambridge University Press, Cambridge, UK and New York, NY, USA, 2007.

Sueper, D.: TOF-AMS Software Downloads, accessible via: <http://cires.colorado.edu/jimenez/> (last access: 17 January 2015), 2010.

Trebs, I., Metzger, S., Meixner, F. X., Helas, G., Hoffer, A., Rudich, Y., Falkovich, A. H., Moura, M. A. L., da Silva Jr., R. S., Artaxo, P., Slanina, J., and Andreae, M. O.: The NH_4^+ - NO_3^- - Cl^- - SO_4^{2-} - H_2O aerosol system and its gas phase precursors at a pasture site in the Amazon Basin: how relevant are mineral cations and soluble organic acids?, *J. Geophys. Res.*, 110, D07303, doi:10.1029/2004JD005478, 2005.

Watson, J. G.: Visibility: science and regulation, *J. Air Waste Manage. Assoc.*, 52, 628–713, 2002.

Wexler, A. S. and Seinfeld, J. H.: The distribution of ammonium salts among a size and composition dispersed aerosol, *Atmos. Environ.*, 24, 1231–1246, 1990.

Zhao, Y. and Gao, Y.: Acidic species and chloride depletion in coarse aerosol particles in the US east coast, *Sci. Total Environ.*, 407, 541–547, 2008.

Zorn, S. R., Drewnick, F., Schott, M., Hoffmann, T., and Borrmann, S.: Characterization of the South Atlantic marine boundary layer aerosol using an aerodyne aerosol mass spectrometer, *Atmos. Chem. Phys.*, 8, 4711–4728, doi:10.5194/acp-8-4711-2008, 2008.

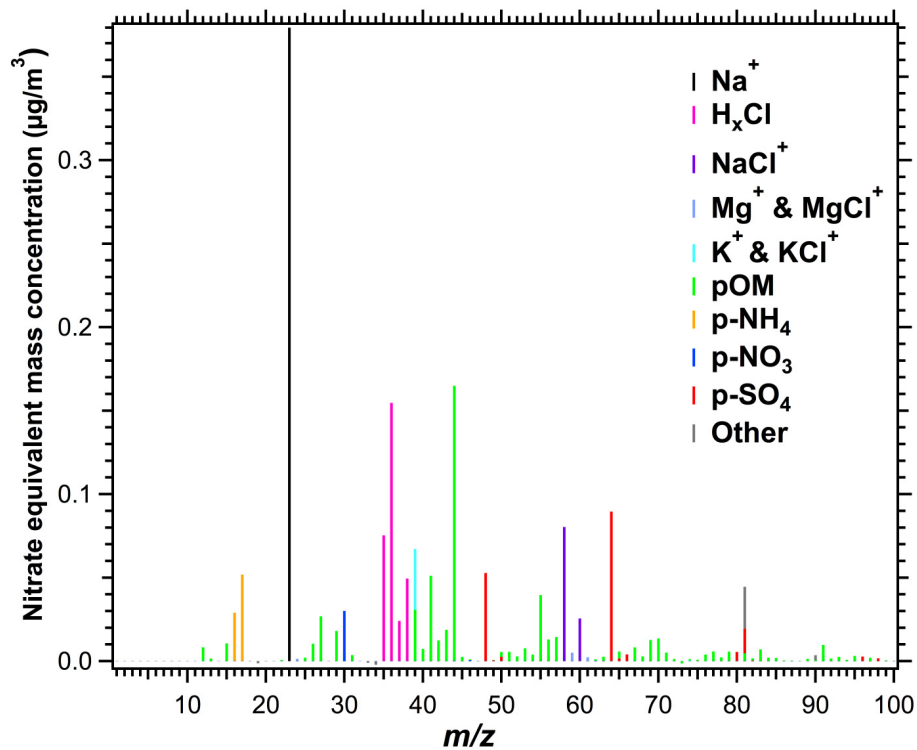


Figure 1. Average aerosol mass spectrum of the Sea Sweep experiments. Air and water peaks were omitted for clarity.

Separating refractory and non-refractory particulate chloride

I. Nuaaman et al.

Title Page	
Abstract	Introduction
Conclusions	References
Tables	Figures
◀	▶
◀	▶
Back	Close
Full Screen / Esc	
Printer-friendly Version	
Interactive Discussion	



Separating refractory and non-refractory particulate chloride

I. Nuaaman et al.

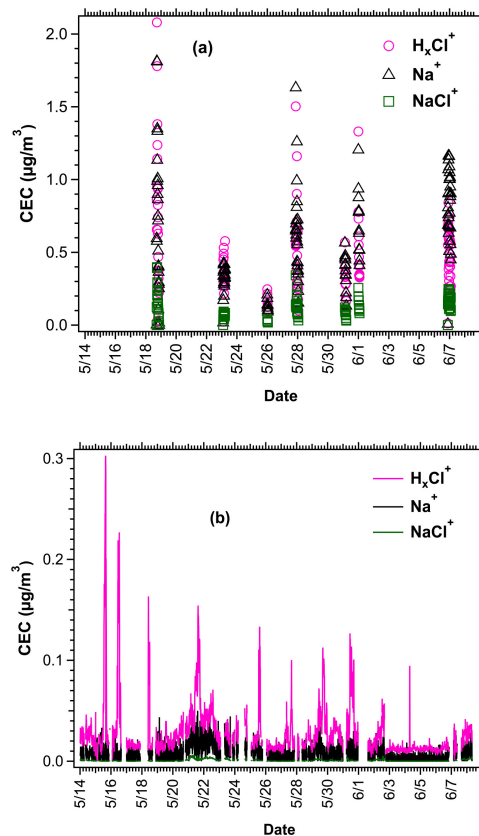


Figure 2. Time series of chloride equivalent concentration signals using an AMS during: **(a)** Sea Sweep experiments **(b)** ambient air.

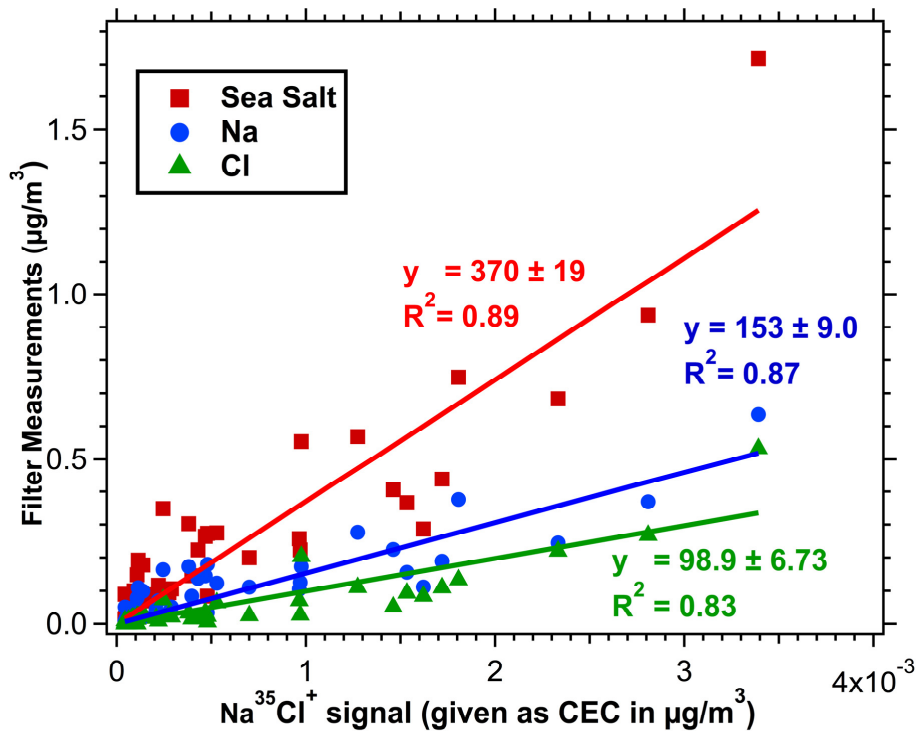


Figure 3. Comparison of submicron filter measurements of sea salt aerosol components and the $\text{Na}^{35}\text{Cl}^+$ signal measured by the HR-AMS.

Separating refractory and non-refractory particulate chloride

I. Nuaaman et al.

Title Page	
Abstract	Introduction
Conclusions	References
Tables	Figures
◀	▶
◀	▶
Back	Close
Full Screen / Esc	
Printer-friendly Version	
Interactive Discussion	



Separating refractory and non-refractory particulate chloride

I. Nuaaman et al.

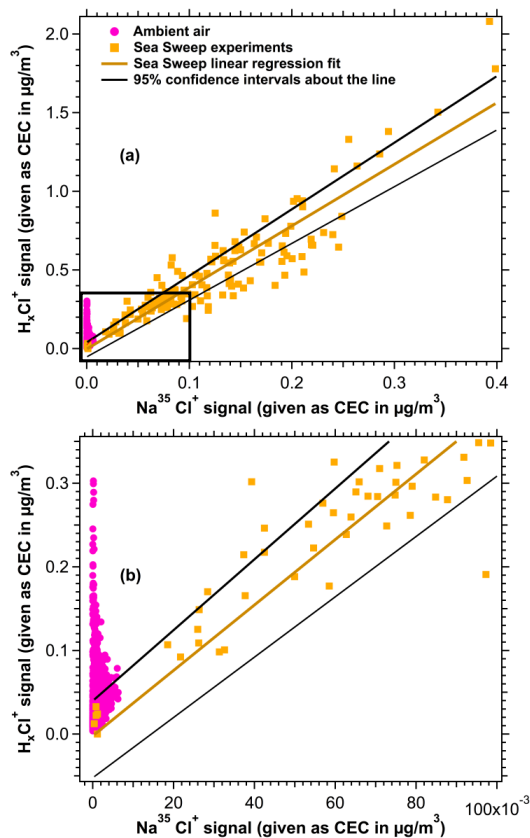


Figure 4. Correlation of H_xCl^+ and $\text{Na}^{35}\text{Cl}^+$ in ambient air and sea sweep experiments. **(b)** is a blow up of the area indicated by the expansion box in **(a)**.

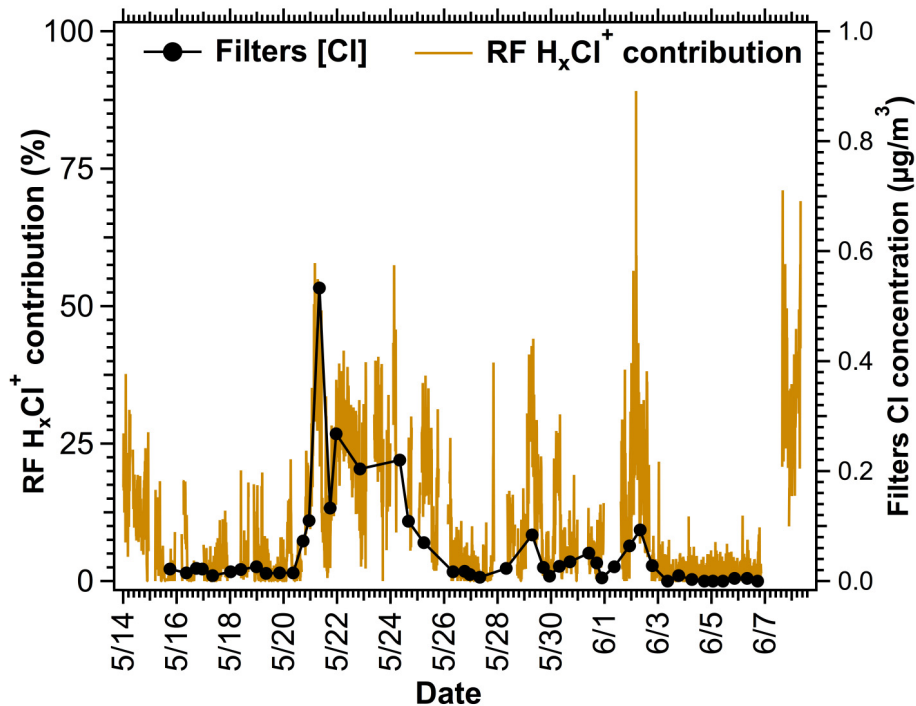


Figure 5. Contribution of refractory H_xCl^+ signal to the total H_xCl^+ signal in ambient air. Chloride concentration determined using filter measurements is shown for comparison.

Separating refractory and non-refractory particulate chloride

I. Nuaaman et al.

Title Page	
Abstract	Introduction
Conclusions	References
Tables	Figures
◀	▶
◀	▶
Back	Close
Full Screen / Esc	
Printer-friendly Version	
Interactive Discussion	



Separating refractory and non-refractory particulate chloride

I. Nuaaman et al.

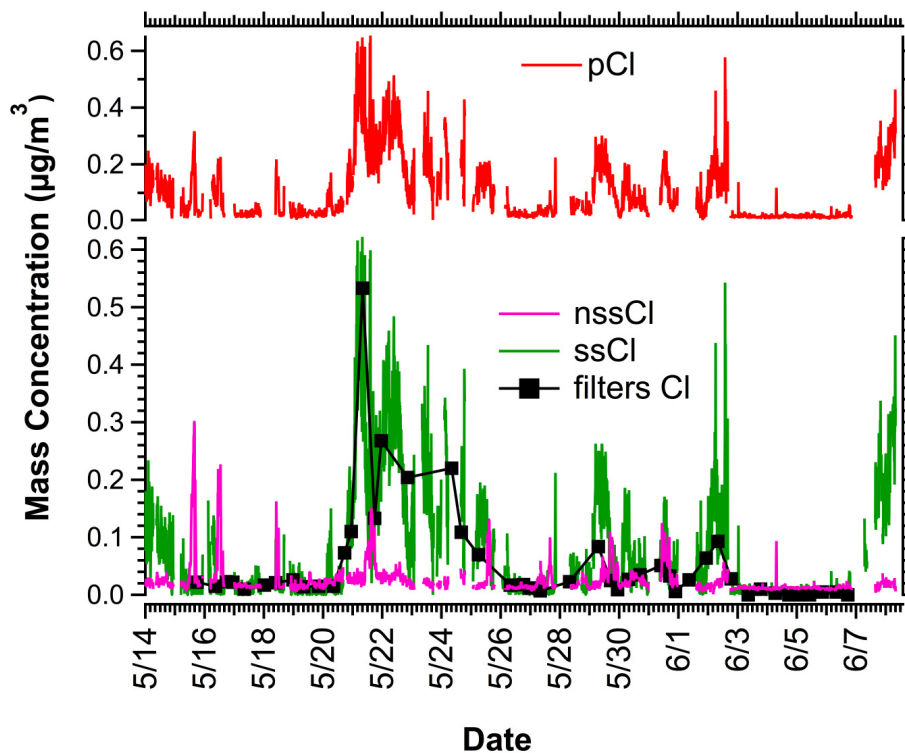


Figure 6. Time series of AMS measurements for pCl, nssCl and ssCl. Filter measurements of submicron [Cl⁻] are also shown for comparison.

[Title Page](#)[Abstract](#)[Introduction](#)[Conclusions](#)[References](#)[Tables](#)[Figures](#)[◀](#)[▶](#)[◀](#)[▶](#)[Back](#)[Close](#)[Full Screen / Esc](#)[Printer-friendly Version](#)[Interactive Discussion](#)

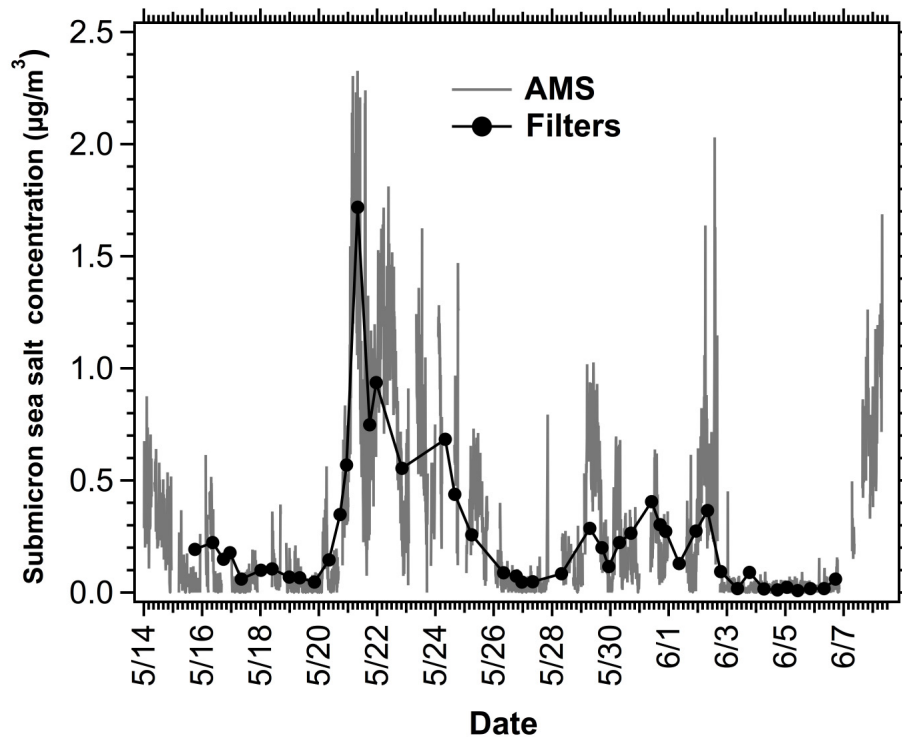


Figure 7. Submicron sea salt concentrations observed during CalNex determined from AMS and filter measurements.

Separating refractory and non-refractory particulate chloride

I. Nuaaman et al.

Title Page	
Abstract	Introduction
Conclusions	References
Tables	Figures
◀	▶
◀	▶
Back	Close
Full Screen / Esc	
Printer-friendly Version	
Interactive Discussion	



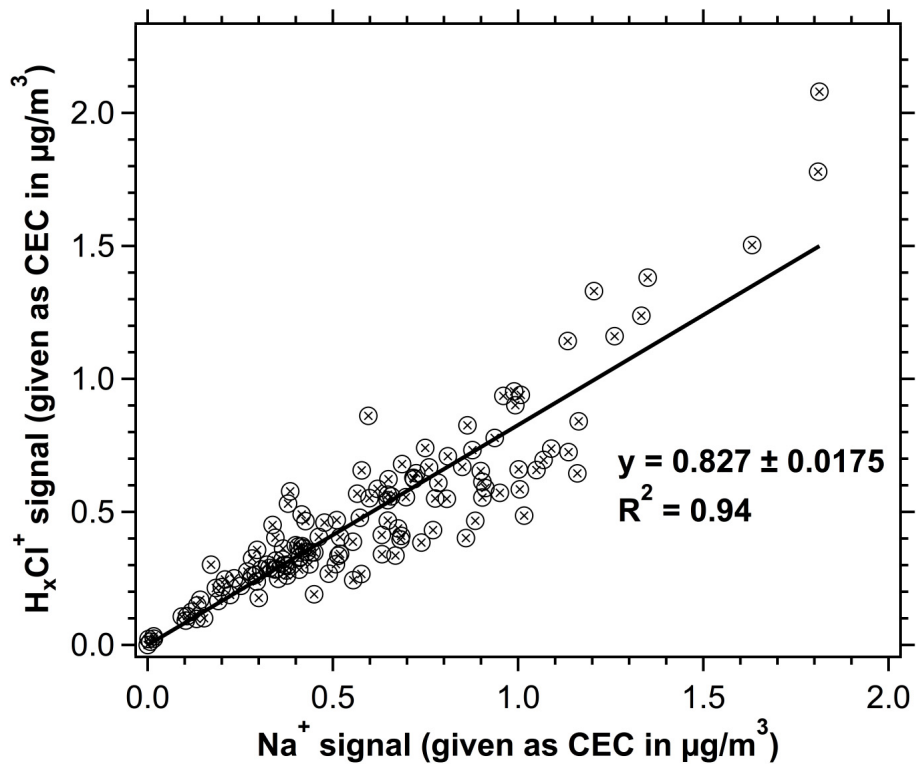


Figure 8. H_xCl^+ to Na^+ signal ratio in Sea Sweep experiments.

Separating refractory and non-refractory particulate chloride

I. Nuaaman et al.

Title Page

Abstract

Introduction

Conclusions

References

Tables

Figures

◀

▶

◀

▶

Back

Close

Full Screen / Esc

Printer-friendly Version

Interactive Discussion



Separating refractory and non-refractory particulate chloride

I. Nuaaman et al.

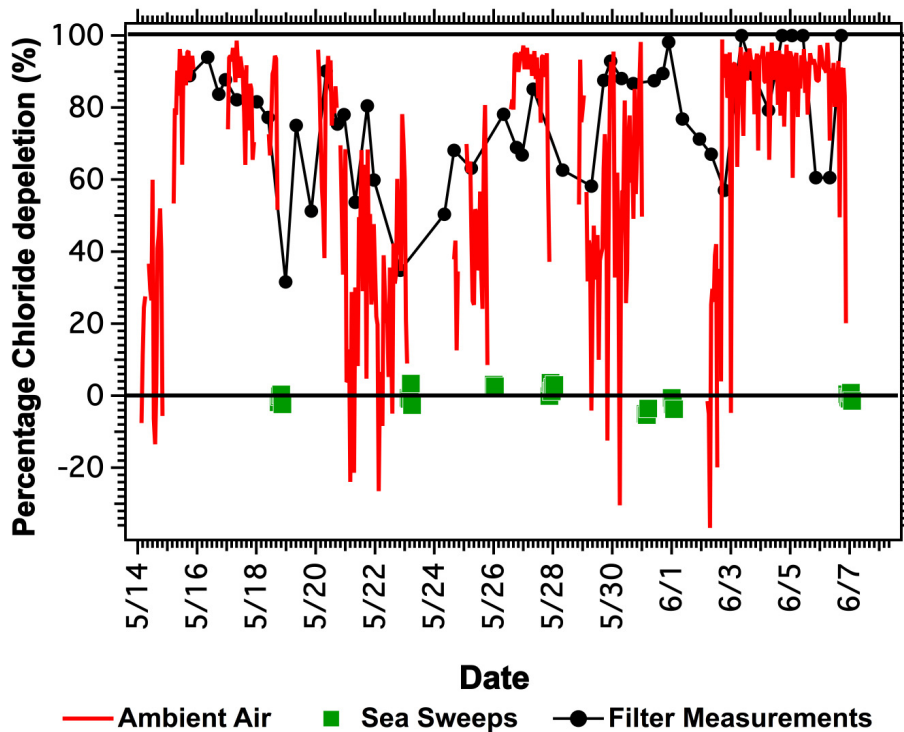


Figure 9. Time series for percentage chloride depletion in submicron aerosols calculated from AMS measurements using Eq. (7). Also shown for comparison is chloride depletion calculated from filter measurements using Eq. (6).